www.elsevier.nl/locate/jorganchem

Journal of Organometallic Chemistry 611 (2000) 52–63

Journal of Organometallic Chemistry

Review

Syntheses, structures, and properties of ladder oligosilanes and ladder oligogermanes

Hideyuki Matsumoto [a],*, Soichiro Kyushin [a], Masafumi Unno [a], Ryoji Tanaka [b]

[a] *Department of Applied Chemistry, Faculty of Engineering, Gunma University, Kiryu, Gunma 376-8515, Japan*
[b] *Gunma University Satellite Venture Business Laboratory, Kiryu, Gunma 376-8515, Japan*

Received 10 April 2000; accepted 22 April 2000

Abstract

Annelated silicon ring systems have received extensive investigation as interesting targets that provide access to physical and chemical properties that are difficult to achieve with the corresponding carbon systems. The aim of this article is to describe the results of our investigation on the chemical and physical properties of the ladder oligosilanes and the ladder oligogermanes, such as bicyclo[2.2.0]hexasilane, tricyclo[4.2.0.$0^{2,5}$]octasilane, tetracyclo[4.4.0.$0^{2,5}$.$0^{7,10}$]decasilane, pentacyclo[6.4.0.$0^{2,7}$.$0^{3,6}$.$0^{9,12}$]-dodecasilane, bicyclo[2.2.0]hexagermane, and tricyclo[4.2.0.$0^{2,5}$]octagermane systems. Such compounds can be prepared by the reductive coupling of the appropriate polychlorosilanes or polychlorogermanes with lithium or magnesium. The X-ray structural analyses of these compounds provide intriguing information about the stereochemistry of the multifused ring systems; each cyclotetrasilane ring or cyclotetragermane ring is not planar but folded, leading to a helical structure of the ladder frameworks of the *anti* type. The ladder oligosilanes and oligogermanes show absorption in the UV–vis region and have considerably low oxidation potentials. The following examples of the reactions of the ladder compounds are described: the ring-opening chlorination, mono- and polyoxidation, and reduction with alkali metals leading to stable radical ions. In addition, chiral symmetry breaking in the *anti*-tricyclo[4.2.0.$0^{2,5}$]octasilane is described. For the reactions of ladder oligosilanes, the comparison with octasilacubanes is also discussed. © 2000 Elsevier Science S.A. All rights reserved.

Keywords: Ladder oligosilane; Ladder oligogermane; Synthesis; Molecular structures; Ring-opening reactions; Photolysis; Chiral crystallization

1. Introduction

The rapid growth of the chemistry of polycyclic compounds of Group 14 elements, Si, Ge, and Sn in the past 15 years has stimulated interest amongst both experimental and theoretical chemists. The versatility of these elements as a structural element in the construction of cyclic molecules has encouraged several research groups to attempt to construct annelated ring systems of Si, Ge, and Sn. During the course of our investigation on the chemistry of small-membered cyclooligosilanes [1], we prepared the first bicyclo[2.2.0]hexasilane, $[RSiSiR][R_2SiSiR_2]_2$ (R = *i*-Pr) (**1**) [2] and the first octasilacubane $[(t\text{-}BuMe_2Si)Si]_8$ [3] and the alkyl-substituted octasilacubane $(ThexSi)_8$ (Thex = 1,1,2-trimethylpropyl) [4]. We have thus studied the chemical and physical properties of oligosilanes and oligogermanes with ladder and cage structures. In this article, we describe the results of our investigation on the chemistry of the ladder oligosilanes and ladder oligogermanes.

The reviews about cyclooligosilanes were written by West in 1982 and 1989 [5], Masamune et al. in 1991 [6], and Hengge and Janoschek in 1995 [7]. The synthesis, structures, and optical properties of ladder oligosilanes and octasilacubanes were reviewed previously by Kyushin et al. in 1994 [8]. In addition, reviews of the chemistry of cage and cluster compounds of Si, Ge, and Sn were written by Sekiguchi and Sakurai in 1992 and 1995 [9]. In addition, the recent advances in the theoretical and experimental aspects of the polyhedranes of Si,

---

* Corresponding author. Fax: +81-277-301291.
E-mail address: matumoto@chem.gunma-u.ac.jp (H. Matsumoto).

PII: S0022-328X(00)00299-0

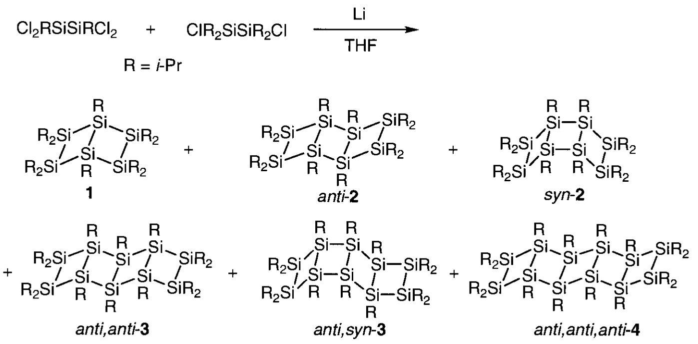

Scheme 1.

Ge, and Sn (e.g. octasilacubanes, hexasilaprismanes, and tetrasilatetrahedrane) were surveyed by Sekiguchi and Nagase in 1998 [10].

2. Ladder oligosilanes

It was not until 1972 that the chemistry of polycyclic ring systems of Si, Ge, and Sn began to start; West and Indriksons reported that the action of Na/K alloy upon a mixture of dimethyldichlorosilane and methyltrichlorosilane in the presence of naphthalene led to the formation of bicyclic and cage oligosilanes [11]. The chemistry of the bicyclic ring systems has then developed systematically, and bicyclo[1.1.0]tetrasilane, bicyclo[1.1.1]pentasilane, bicyclo[2.2.0]hexasilane, bicyclo[2.2.2]octasilane, bicyclo[2.2.1]heptasilane, bicyclo[4.2.0]octasilane, bicyclo[3.3.0]octasilane, bicyclo[4.4.0]decasilane, bicyclo[2.2.0]hexastannane, and bicyclo[1.1.1]pentastannane systems are now known [5–14].

In carbon systems, ladderanes which have multifused cyclobutane rings, some examples of chromophore-appended, fully saturated rigid ladder oligomers and polymers have been reported recently [15]. These rigid, fully saturated backbones are expected to be useful scaffolds onto which antenna chromophores might be affixed and would provide interesting modes for understanding long distance interchromophore interactions along the σ(C–C) bond framework [15d].

Since the synthesis of the bicyclo[2.2.0]hexasilane [2], we have directed our attention to the ladder oligosilanes and oligogermanes, since it has been expected that such molecules possess intriguing chemical and physical properties arising from extension of Si–Si σ-electron delocalization as well as ring strain.

2.1. Syntheses

We found that the multifused cyclotetrasilane rings can be constructed by cross-coupling of Cl_2(*i*-Pr)SiSi(*i*-Pr)Cl_2 and Cl(*i*-Pr)$_2$SiSi(*i*-Pr)$_2$Cl with lithium in tetrahydrofuran (THF) [2,8,16]. By coupling, a mixture of the bicyclo[2.2.0]hexasilane [(*i*-Pr)SiSi(*i*-Pr)][(*i*-Pr)$_2$SiSi(*i*-Pr)$_2$]$_2$ (**1**), *anti*- and *syn*-tricyclo[4.2.0.0^{2,5}]octasilanes [(*i*-Pr)SiSi(*i*-Pr)]$_2$[(*i*-Pr)$_2$SiSi(*i*-Pr)$_2$]$_2$ (*anti*-**2** and *syn*-**2**), *anti,anti*- and *anti,syn*-tetracyclo[4.4.0.0^{2,5}.0^{7,10}]decasilanes [(*i*-Pr)SiSi(*i*-Pr)]$_3$[(*i*-Pr)$_2$SiSi(*i*-Pr)$_2$]$_2$ (*anti,anti*-**3** and *anti,syn*-**3**) and *anti,anti,anti*-pentacyclo[6.4.0.0^{2,7}.0^{3,6}.0^{9,12}]dodecasilane [(*i*-Pr)SiSi(*i*-Pr)]$_4$[(*i*-Pr)$_2$SiSi(*i*-Pr)$_2$]$_2$ (*anti,anti,anti*-**4**), and higher oligomers was produced (Scheme 1). Each ladder oligosilane can be separated by use of chromatographic methods (a preparative reversed-phase HPLC) as colorless (**1** and *anti*-**2**) and yellow (*syn*-**2**, *anti,anti*-**3**, *anti,syn*-**3**, and *anti,anti,anti*-**4**) crystals.

In the cross-coupling, the product distribution can be controlled by the ratio of the two chlorodisilanes. For example, by using a large excess of 1,2-dichloro-1,1,2,2-tetraisopropyldisilane, bicyclohexasilane **1** is obtained preferentially. On the other hand, the reaction with a large excess of 1,1,2,2-tetrachloro-1,2-diisopropyldisilane resulted in the preferential formation of higher oligomers such as *anti,anti*-**3**, *anti,syn*-**3** and *anti,anti,anti*-**4**.

We have also found that the *all*-*trans*-tetrachlorocyclotetrasilane [Cl(*t*-Bu)Si]$_4$ is a convenient precursor for the construction of the tricyclo[4.2.0.0^{2,5}]octasilane framework [17]. The compound [Cl(*t*-Bu)Si]$_4$ can be prepared via the chlorodephenylation of stereoisomeric mixtures of the cyclotetrasilane [Ph(*t*-Bu)Si]$_4$ [1g]. Thus, the reductive coupling of [Cl(*t*-Bu)Si]$_4$ with Cl(*i*-Pr)$_2$SiSi(*i*-Pr)$_2$Cl with lithium produces *anti*-tricyclo[4.2.0.0^{2,5}]octasilane [(*t*-Bu)SiSi(*t*-Bu)]$_2$[(*i*-Pr)$_2$SiSi(*i*-Pr)$_2$]$_2$ (**5**) in 40% yield [17] (Scheme 2). In this

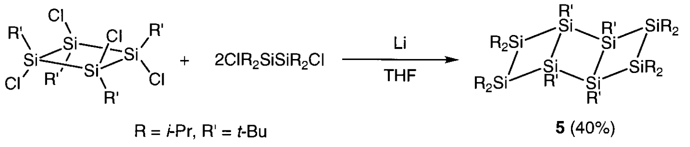

Scheme 2.

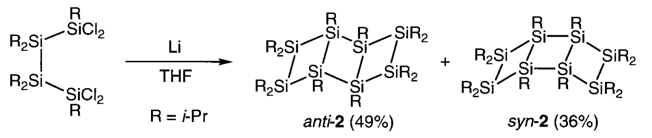

Scheme 3.

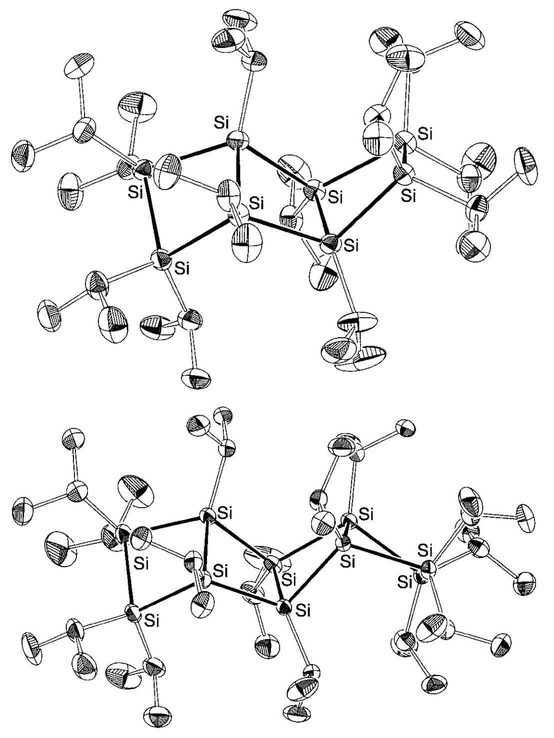

Fig. 1. Crystal structures of *anti*-**2** and *anti,anti*-**3**. Thermal ellipsoids are drawn at the 30% probability level.

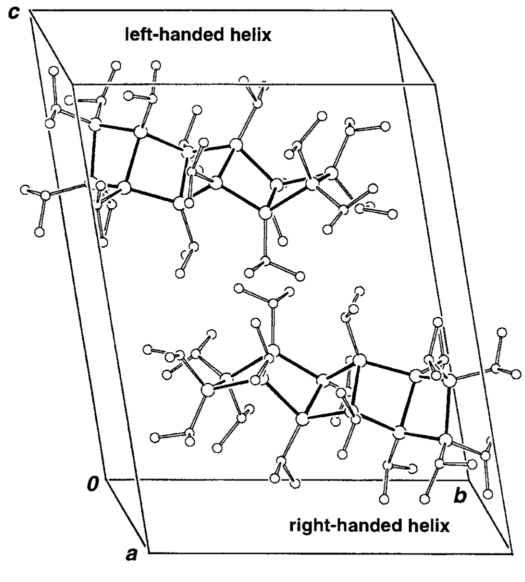

Fig. 2. Packing drawing of *anti,anti,anti*-**4** in a centric unit cell.

coupling reaction, the *syn* isomer was not formed under the conditions employed.

It is noted that the perisopropyltricyclooctasilanes, *anti*-**2** and *syn*-**2**, can also be synthesized by the homocoupling of the 1,1,4,4-tetrachlorotetrasilane Cl_2-(i-Pr)Si[(i-Pr)$_2$Si]$_2$Si(i-Pr)Cl_2 with lithium in 49 and 36% yields, respectively [18] (Scheme 3).

2.2. Molecular structures

The structures of the ladder oligosilanes were confirmed by X-ray crystallography. In bicyclohexasilane **1**, cyclotetrasilane rings are connected in a *cis*-fused configuration. Each cyclotetrasilane ring is not planar but folded with fold angles of 21.4–21.8° [2b], whereas MO calculation of the Si_6H_{10} compound led to a planar structure with C_{2v} symmetry [19]. The central Si–Si bond distance (2.396(2) Å) in **1** is comparable with peripheral Si–Si bond distances (2.385(2)–2.426(2) Å).

It is noteworthy that the structures of ladder oligosilanes are highly affected by their stereochemistry. In the tricyclo[4.2.0.0^{2,5}]octasilane, the Si–Si bond distances of *anti*-**2** range from 2.346(3) to 2.405(4) Å with an average of 2.388 Å. The fold angles of three cyclotetrasilane rings are 22.6–25.2°. The dihedral angles between neighboring cyclotetrasilane rings are 111.4–112.8°. On the other hand, *syn*-**2** has a more distorted structure. The Si–Si bond distances (2.369(4)–2.436(4) Å, average 2.402 Å) are longer than those of *anti*-**2**. The cyclotetrasilane rings have more planar structures with fold angles of 10.0–21.0°. The dihedral angles between neighboring cyclotetrasilane rings are 118.8–129.5°. Apparently, relatively crowded *syn*-**2** prefers the longer Si–Si bond distances and the more planar cyclotetrasilane rings to minimize the steric repulsion among the isopropyl groups. Similar structural features are observed in *anti,anti*-**3** and *anti,syn*-**3**. The structural parameters of *anti,anti*-**3** are quite similar to those of *anti*-**2**. In *anti,syn*-**3**, the *syn* moiety consisting of three cyclotetrasilane rings has a similar structure to *syn*-**2** and the residual cyclotetrasilane ring has features of *anti*-**2**. The ORTEP drawings of *anti*-**2** and *anti,anti*-**3** are shown in Fig. 1 [8,16].

As seen from Fig. 1, the *anti* ladder oligosilanes (**1**, *anti*-**2**, *anti,anti*-**3** and *anti,anti,anti*-**4**) have a helical structure. These molecules can be seen as silicon double helices, in which two linear oligosilane chains screw in one way and are bridged by Si–Si bonds. Moreover, it is noted that the Si–Si bonds in each chain are repeated with alternating long and short distances. The twist angles between the terminal Si–Si rungs are 44.0° (*anti*-**2**), 63.0° (*anti,anti*-**3**), and 80.3° (*anti,anti,anti*-**4**) [20]. In the case of *anti,anti,anti*-**4**, the X-ray analysis of the single crystal thus obtained showed that left- and right-hand skewed molecules are paired in a unit cell, since the crystal of this ladder oligosilane has a centrosymmetric space group, as shown in Fig. 2 [20]. Therefore, the crystals are racemates of chiral helical molecules. The helical structures are notable because the X-ray crystal structures of the carbon systems [4]- and [5] ladderanes have been reported to have planar cyclobutane rings, which are catenated in a corrugated manner without twist [15c,d,21]. It is obvious that the helical structures of ladder oligosilanes arise from the systematic catenation of folded cyclotetrasilane rings.

2.3. Electronic properties

The ladder oligosilanes have unique electronic properties. They show relatively strong absorption in the UV–vis region [8,16]. In a series of the *anti* isomers, the absorption maxima of the longest wavelength shift to the longer wavelength region as the number of cyclotetrasilane rings progressively increases; **1**: 310 nm, *anti*-**2**: 345 nm, *anti*,*anti*-**3**: 380 nm, *anti*,*anti*,*anti*-**4**: 414 nm. A similar bathochromic shift was reported in permethyloligosilanes and the shift is explained by the extension of σ-conjugation of the Si–Si bonds [22]. The absorptions of *syn* ladder oligosilanes extend to the longer wavelength region in comparison to those of the corresponding *anti* isomers. For example, the absorption maximum of the longest wavelength exists at 398 nm in *syn*-**2**. The observed trend is explained in terms of the destabilized highest occupied molecular orbital (HOMO) of the *syn* isomers because of the more strained oligosilane skeletons than those of the *anti* isomers.

The ladder oligosilanes exhibit a highly electron-donating property. The oxidation potentials measured by cyclic voltammetry range from 0.51 to 0.87 V versus SCE in CH_2Cl_2 [8,16]. The oxidation potentials show several interesting features. The oxidation potentials of *anti* ladder oligosilanes slightly decrease as the number of cyclotetrasilane rings increases. Since oxidation potentials are mainly related to the energy levels of the HOMO, the decrease of oxidation potentials is explained in terms of the destabilization of the HOMO by the extension of σ-conjugation. Another feature is that *syn* ladder oligosilanes show far lower oxidation potentials than those of the corresponding *anti* isomers (e.g. 0.51 V in *syn*-**2** vs. 0.85 V in *anti*-**2**). The low oxidation potentials of the *syn* isomers are attributable to the destabilization of the HOMO by the highly strained *syn* structure and the results are in good accord with the tendency observed in the UV–vis spectra. It is noted that the octasilacubanes $[(t\text{-BuMe}_2\text{Si})\text{Si}]_8$ and $(\text{ThexSi})_8$ have significantly low oxidation potentials of ca. 0.4 V versus SCE [3,4].

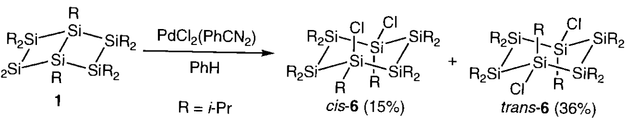

Scheme 4.

2.4. Reactions

2.4.1. Ring-opening chlorination

Owing to their low oxidation potentials, the ladder oligosilanes are highly reactive toward electrophiles. When bicyclo[2.2.0]hexasilane **1** was allowed to react with $PdCl_2(PhCN)_2$ in benzene at room temperature (r.t.), 1,4-dichlorodecaisopropylcyclohexasilanes (**6**) was formed as a mixture of *cis* and *trans* isomers; yields of *cis*-**6** and *trans*-**6** were 15 and 36%, respectively [23] (Scheme 4).

These 1,4-dichlorocyclohexasilanes exhibit remarkable structural features and reactivity that have not been observed with other 1,4-dichlorohexasilane systems [23]. The X-ray structural analysis indicates that the cyclohexasilane rings of both isomers exist in distorted chair conformations. The Si–Si bond distances of *cis*-**6** (2.403(3)–2.422(2) Å) and *trans*-**6** (2.416(1)–2.418(1) Å) are longer than those of cyclohexasilanes so far reported, due to the steric repulsion among the isopropyl groups [23]. In *trans*-**6**, both chlorine atoms occupy equatorial positions and the geminal isopropyl groups occupy axial positions. The conformation observed in *trans*-**6** is explained by the fact that the 1,3-diaxial interaction among the isopropyl groups may not be very important because of the long length of the Si–Si bonds. Moreover, if the isopropyl groups occupied equatorial positions, the steric repulsion among the isopropyl groups and four vicinal isopropyl groups would be significantly large because of the *gauche* conformation. The result is also confirmed by the MM2 calculation that the conformation of the equatorial-Cl and axial-*i*-Pr is more stable than that of the axial-Cl and equatorial-*i*-Pr in *trans*-**6** [23]. The UV spectra of *cis*-**6** and *trans*-**6** are noteworthy. The absorptions corresponding to the lowest-energy transitions appear at ca. 285 nm (ε 1600) in *cis*-**6** and at ca. 280 nm (ε 1300) in *trans*-**6**. The absorption bands shift to the longer wavelength region and have larger extinction coefficients in the order of dodecamethylcyclohexasilane < *trans*-**6** < *cis*-**6**. The order is in agreement with their strain energies and explained by the fact that the strained Si_6 skeleton has the high energy of the HOMO.

Interestingly, in *cis*-**6** and *trans*-**6**, a transannular reaction occurred to quantitatively reproduce bicyclohexasilane **1** by the reductive coupling with sodium under reflux in toluene (Scheme 5) [23]. The intermolecular coupling products were not formed under these conditions, indicating the rapid intramolecular coupling. The result is in contrast with that of dichlorodecamethylcyclohexasilanes, in which only intermolecular coupling occurs [24]. The reaction is also unique be-

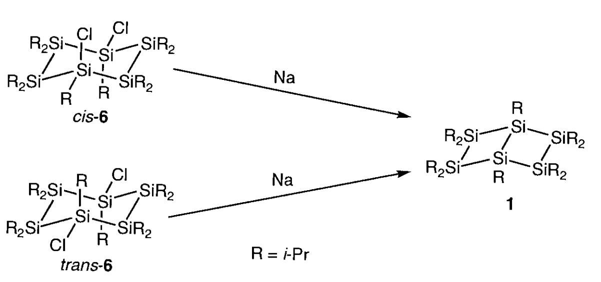

Scheme 5.

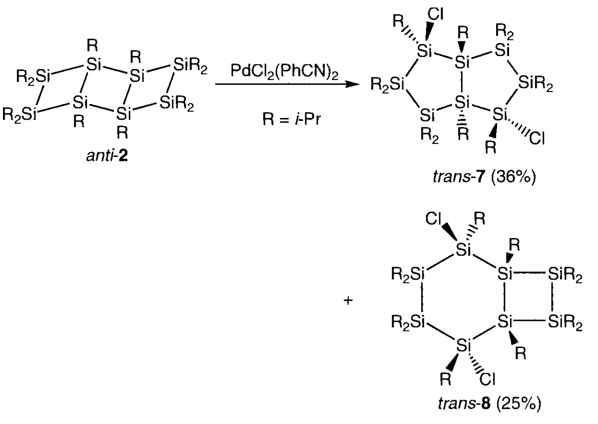

Scheme 6.

cause the stereochemistry of dichlorocyclohexasilane **6** does not influence the course of the reaction, although details of the mechanism for the stereochemistry cannot be explained at that moment. Probably, the role of isopropyl groups is important for the transannular reaction. The intramolecular steric repulsion among the isopropyl groups on the cyclohexasilane ring facilitates the formation of the bicyclo[2.2.0]hexasilane ring and the intermolecular steric repulsion among the isopropyl groups suppresses the coupling reaction of two molecules of **6**.

The reaction of the tricyclo[4.2.0.0^{2,5}]octasilane *anti*-**2** with a small excess of $PdCl_2(PhCN)_2$ in benzene under reflux led to the formation of *trans*-2,6-dichlorododecaisopropylbicyclo[3.3.0]octasilane (*trans*-**7**) and *trans*-2,5-dichlorododecaisopropylbicyclo[4.2.0]octasilane (*trans*-**8**) in 36 and 25% yields, respectively (Scheme 6) [25]. The formation of *trans*-**7** shows that both bridgehead Si–Si bonds of *anti*-**2** were cleaved and rearranged to the bicyclo[3.3.0]octasilane system, while in *trans*-**8**, one of the bridgehead Si–Si bonds of *anti*-**2** was simply cleaved to form the bicyclo[4.2.0]octasilane system. X-ray crystallography shows that the bicyclo[3.3.0]-octasilane framework of *trans*-**7** has the *trans*-fused structure of cyclopentasilane rings [25]. The *trans*-fused structure is notable because, in bicyclo[3.3.0]octane, the *cis*-fused structure has been shown to be more stable than the *trans*-fused structure [26]. In fact, the MM2 calculations show that the *cis*-fused isomer of *trans*-**7** is more stable than *trans*-**7** itself. Therefore, the ring-opening reaction is considered to be kinetically controlled.

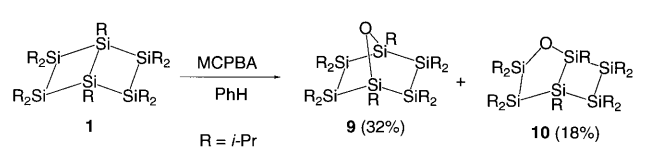

Scheme 8.

The ring-opening reaction of *anti*-**2** with PCl_5 gives *cis*- and *trans*-2,5-dichlorododecaisopropylbicyclo-[4.2.0]octasilane (*cis*-**8** and *trans*-**8**) in 47 and 11% yields, respectively (Scheme 7) [25]. In this reaction, the bridgehead Si–Si bonds of *anti*-**2** are also highly reactive toward PCl_5. However, rearrangement products such as *trans*-**7** were not formed, and *cis*-**8** was produced in preference to *trans*-**8** in contrast with the reaction using the palladium complex. These results seem to reflect different mechanisms in the ring-opening reactions of *anti*-**2** with $PdCl_2(PhCN)_2$ and PCl_5.

2.4.2. Oxidation of Si–Si bonds

Oxidation of Si–Si bonds with peroxy acids has been known to be one of the fundamental reactions of oligo- and polysilanes [27]. We found that the oxidation of bicyclo[2.2.0]hexasilane **1** with a deficient amount (0.7 equivalent) of *m*-chloroperbenzoic acid (MCPBA) gave decaisopropyl-7-oxabicyclo[2.2.1]heptasilane (**9**) (32%) and decaisopropyl-2-oxabicyclo[3.2.0]heptasilane (**10**) (18%) as mono-oxidation products (Scheme 8) [28]. In the UV spectrum of **9**, the absorption maximum of the longest wavelength (313 nm) exists almost in the same position as that of **1** (310 nm), and the extinction coefficient (ε 5100) is fairly large. The observed trend is quite remarkable in light of prior reports that insertion

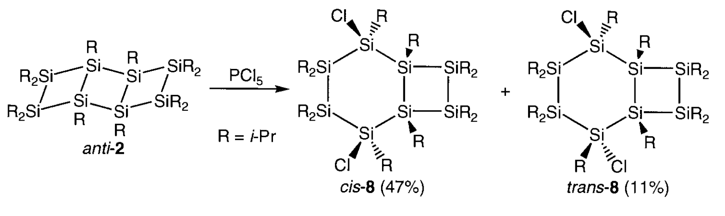

Scheme 7.

of an oxygen atom into catenated silicon atoms interrupts σ conjugation and results in the hypsochromic shift in the absorption spectrum. On the other hand, the UV spectrum of the 2-oxa compound **10** does not show such unique absorption and resembles that of **1**, indicating that the absorption spectra strongly depend on the position of the oxygen atom in the Si$_6$O framework. Therefore, the unique absorption bands of **9** seem to be due to the stereoelectronic effect of the oxygen atom at the 7-position. The ab initio calculation (STO-3G) indicated that the lobes of the HOMO and the next HOMO of **9** are delocalized in both lone pairs of the oxygen atom and the peripheral Si–Si bonds and that the n orbital interacts with Si–Si σ bonds and the novel σ–n conjugation may be the origin of the new absorption bands of **9**. Compound **9** also shows far stronger fluorescence than that of the bicyclo[2.2.0]hexasilane; the strong fluorescence corresponds to the relatively large extinction coefficient in the UV spectrum [28].

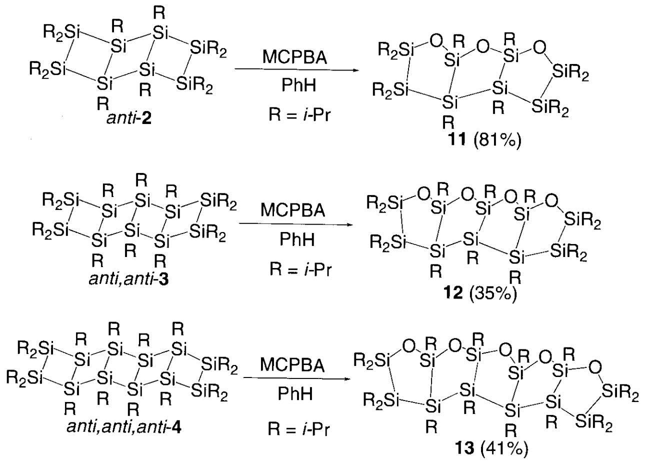

Scheme 9.

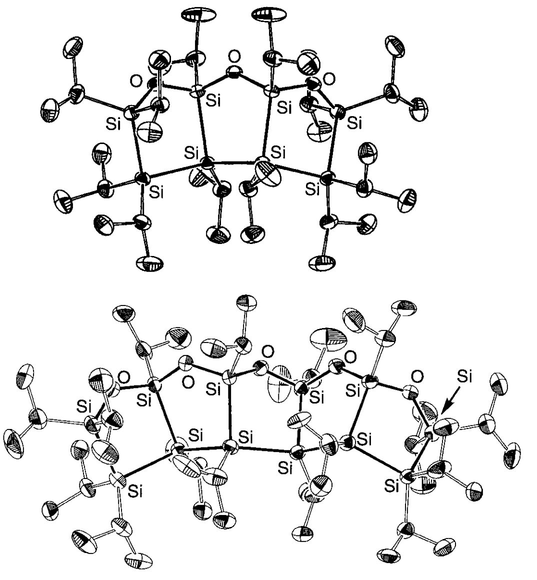

Fig. 3. Crystal structures of trioxide **11** (top) and pentaoxide **13** (bottom). Thermal ellipsoids are drawn at the 30% probability level.

Polyoxidation of the ladder oligosilanes exhibits unique regioselectivity; the domino oxidation of the Si–Si bonds takes place to produce novel ladder polyoxa compounds. When *anti*-dodecaisopropyltricyclo[4.2.0.0^{2,5}]octasilane (*anti*-**2**) was oxidized with three equivalents of MCPBA, the trioxide **11** was obtained in 81% yield [29]. Similarly, the oxidation of *anti,anti*-tetradecaisopropyltetracyclo[4.4.0.0^{2,5}.0^{7,10}]decasilane (*anti,anti*-**3**), and *anti,anti,anti*-hexadecaisopropylpentacyclo[6.4.0.0^{2,7}.0^{3,6}.0^{9,12}]dodecasilane (*anti,anti,anti*-**4**) with four and five equivalents of MCPBA yielded tetraoxide **12** and pentaoxide **13**, respectively, in moderate yields (Scheme 9) [29]. Therefore, the ladder oligosilanes were found to be oxidized in a quite unique manner; one of two Si–Si chains is oxidized selectively, and novel ladder compounds consisting of oligosiloxane and oligosilane chains were formed. As far as we know, the compounds such as **11**, **12**, and **13** have not been reported in carbon analogs.

The X-ray crystallography disclosed that these polyoxides molecules have a curved shape containing an oligosiloxane chain as an outer arch and an oligosilane chain as an inner arch. They retain the *anti* structure of the starting ladder oligosilanes, and each five-membered ring is catenated in a corrugated manner. Furthermore, the corrugated arch is twisted as shown in Fig. 3. The twisted structures arise from the systematic catenation of the five-membered rings, which have an intermediate structure between the envelope and twist forms. The Si–Si bonds of the inner oligosilane chain are significantly long (trioxide **11**: 2.398(2)–2.409(2) Å, tetraoxide **12**: 2.404(3)–2.420(3) Å, pentaoxide **13**: 2.389(2)–2.434(3) Å), while the other Si–Si bond lengths are rather normal (**11**: 2.388(2)–2.390(2) Å, **12**: 2.375(3)–2.395(3) Å, **13**: 2.390(3)–2.410(2) Å) [29]. The enlarged steric repulsion among the isopropyl groups of the inner oligosilane chain, which is caused by the introduction of oxygen atoms to the opposite chain, seems to be the origin of the elongation of the Si–Si bonds.

There are several significant features of this polyoxidation. Only small or negligible amounts of intermediate oxidation products are detected during the reactions. For example, in the case of the tricyclooctasilane *anti*-**2**, the intermediate mono- and dioxidation products were not detected even during the initial stage of the reaction, but **11** was formed instead. This means that the mono- and dioxidation products are highly activated toward oxidation, and are immediately oxidized to **11** after they are formed. The positional selectivity observed during the oxidation may be explained in terms of a significant enhancement of the reactivity of the Si–Si bonds adjacent to the oxygen due to an

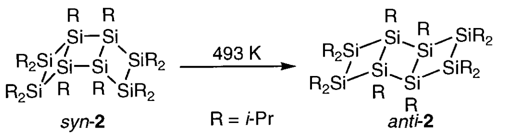

Scheme 10.

electronic effect, as well as hydrogen bonding of MCPBA to the siloxane oxygen, which brings the peracid into close proximity with the adjacent Si–Si bonds [27g,h]. When all the Si_4 rings were oxidized to the Si_4O rings, further oxidation did not proceed under the conditions employed and the polyoxidation products containing an oxygen atom in each ring were obtained. Apparently, release of the strain energy on the Si_4 rings seems to be another driving force of this particular polyoxidation.

The oxidation products **11**, **12**, and **13** are interesting from the viewpoint of their electronic properties. They exhibit intense absorptions in the UV region, and, as the number of the Si_4O rings increases, the absorption maxima of the longest wavelengths show a bathochromic shift, and the molecular extinction coefficient becomes far greater (**11**: 273 nm (ε 7600), **12**: 292 nm (ε 25000), **13**: 297 nm (ε 51900)). The intense absorption in the order 10^4 is remarkable because these molecules contain no chromophores, which give such an intense absorption. Since the intense absorption is not observed in the ladder oligosilanes, it is apparently due to the electronic effect of the oxygen atoms on the Si–Si σ conjugation systems [29].

2.4.3. Thermolysis and photolysis

When heated at 493 K, *syn*-tricyclooctasilane *syn*-**2** isomerizes to *anti*-tricyclooctasilane *anti*-**2** (Scheme 10); isomerization of *anti*-**2** to *syn*-**2** does not occur at 493 K. Thermodynamic parameters were determined for the one-way isomerization of *syn*-**2** to *anti*-**2**: $E_a = 42.3$ kcal mol^{-1}, $\Delta H^{\ddagger} = 41.4$ kcal mol^{-1}, $\Delta S^{\ddagger} = 7.6 \times 10^{-3}$ kcal mol^{-1} K^{-1} [30]. The activation energy is considerably greater than that for the analogous thermal isomerization of *syn*-tricyclo[4.2.0.0^{2,5}]octane to *anti*-tricyclo[4.2.0.0^{2,5}]octane [31], indicating the bond dissociation energy of the bridgehead Si–Si bond of *syn*-**2** is greater than that of the bridgehead C–C bond of *syn*-tricyclo[4.2.0.0^{2,5}]octane.

The photolysis of tricyclooctasilanes *anti*-**2** and **5** results in the generation of peralkylcyclotetrasilenes, which provides the opportunity for assessing reactivity of the unsaturated Si_4 framework. On irradiation of hexane solutions of *anti*-**2** in the presence of 2,3-dimethyl-1,3-butadiene and anthracene with a high-pressure mercury lamp through a filter, cyclotetrasilane derivatives **15a** and **6** were formed, respectively (Scheme 11) [32]. In these reactions, trap products of dialkylsilylene and tetraalkyldisilene intermediates were not detected. These results indicate that two peripheral Si–Si bonds in the central cyclotetrasilane ring are cleaved selectively to afford two molecules of the cyclotetrasilene intermediate.

The site selectivity in the Diels–Alder reactions of cyclotetrasilenes with anthracene is especially noted. The cycloaddition of **14a** takes place at the 9,10-positions of anthracene according to the frontier orbital theory. However, in the case of **14b**, the cycloaddition at the 9,10-positions is unfavorable because of the steric hindrance between *tert*-butyl groups and a benzene ring. Avoiding such steric hindrance, the cycloaddition of **14b** took place at the 1,4-positions to give **17**. To our knowledge, this is the first example of the Diels–Alder reaction of anthracene at the 1,4-positions [32].

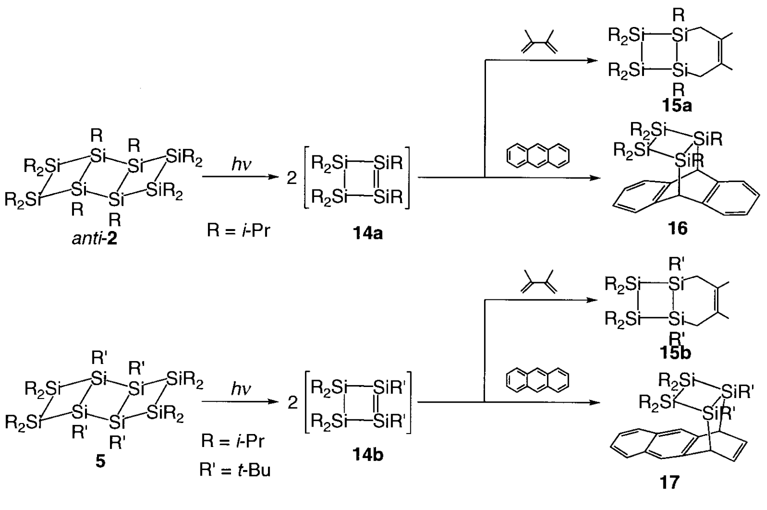

Scheme 11.

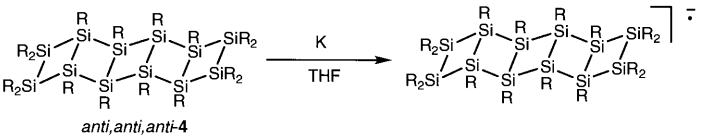

anti,anti,anti-**4**

Scheme 12.

2.4.4. Reduction with alkali metals; formation of stable radical anions

The ladder oligosilanes can be readily reduced by K to generate the radical anions (Scheme 12) [33].

When *anti,anti,anti*-**4** was treated with K mirror at ca. −70°C in degassed THF in a sealed tube, the solution was immediately colored black, indicating that the new absorption appeared in the Vis-NIR region. A remarkable feature of the radical anion of *anti,anti,anti*-**4** is its unusual stability. When the temperature of the radical anion of *anti,anti,anti*-**4** generated at −70°C was raised up to r.t., the black color did not change, and the intensity of the ESR signals did not decrease at all. Furthermore, the ESR signals persisted for several months at r.t. For example, the intensity loss after 1 month is 19%, and the half-life is too long to be measured. The stability is striking because almost all of the radical anions of cyclooligosilanes have been reported to be stable only below ca. −50°C, except for the radical anion of $[(t\text{-Bu})\text{MeSi}]_4$, which persists for several days at r.t. [34]. The unusual stability of the radical anion of *anti,anti,anti*-**4** is explained by the highly delocalized spin, which is protected by bulky substituents. Although many radical anions of oligosilanes have been generated by the reduction with K or Na/K alloy, no examples using Li have been reported to our knowledge compound, *anti,anti,anti*-**4** is reduced even with Li as well as K. The results show that the lowest unoccupied molecular orbital (LUMO) of *anti,anti,anti*-**4** is considerably stabilized by the interaction of Si–Si σ* and Si–C σ* orbitals extended over the molecule.

2.4.5. Chiral crystallization of anti-dodecaisopropyltricyclo[4.2.0.0^{2,5}]octasilane

Since the report of the spontaneous resolution of each enantiomer in crystallization from a racemic solution of $NaClO_3$ in 1990 [35], chiral symmetry breaking has attracted considerable attention from the point of view of absolute asymmetric synthesis and applications based on nonlinear optical and chiroptical properties. Quite recently, Kondepudi and co-workers have reported that chiral symmetry breaking of 1,1′-binaphtyl can be realized in crystallization from a melt by the mere act of stirring [36].

As for the compounds of Group 14 elements, Si, Ge, and Sn, chiral symmetry breaking has not yet been reported except for one case. Thus, in 1995, Weidenbruch and co-workers reported that hexa-*t*-butyl-1,3-diiodotrigermane, produced by the cleavage of hexa-*t*-butylcyclotrigermane with iodine, forms a conglomerate of enantiomerically pure crystals on slow cooling to −25°C. However, the Si analog of the 1,3-diiodide crystallized as a racemate [37]. Recently, the preparation of optically active dialkyl-, alkylaryl- and diarylpolysilanes with preferential screw-sense helical backbone conformations in solution has been achieved through the incorporation of enantiopure chiral side chains or endo groups and their interesting optical properties have been demonstrated [38].

We found that *anti*-tricyclo[4.2.0.0^{2,5}]octasilane *anti*-**2** yields one large crystal of each enantiomer (*M* or *P*) spontaneously upon crystallizing from a solution without stirring. In a total of **13** different crystallizations, six were predominantly enantiomer *M*, while seven were enantiomer *P* (Scheme 13) [39]. Studies on chiral symmetry breaking in the tetracyclic oligosilane (*anti,anti*-**3**) are now under way.

3. Ladder oligogermanes

The ladder oligogermane has not yet been reported except for one case. Thus, Sekiguchi and Sakurai reported in 1994 that the reaction of 1,2,3,4-tetra-*t*-butyl-1,2,3,4-tetrachlorocyclotetragermane with sodium in tetrahydrofuran (THF) had given *anti*-3,4,7,8-tetrachloro-1,2,3,4,5,6,7,8-octa-*t*-butyltricyclo[4.2.0.0^{2,5}]octagermane in 21% yield as well as 4,8-dichloro-1,2,3,4,5,6,7,8-octa-*t*-butyltetracyclo[3.3.0.0^{2,7}.0^{3,6}]octagermane (8%) [40]. Recently, we prepared 1,4-di-*t*-butyl-2,2,3,3,5,5,6,6-octaisopropylbicyclo[2.2.0]hexagermane (**18**) and 1,2,5,6-tetra-*t*-butyl-3,3,4,4,7,7,8,8-octaisopropyl tricyclo[4.2.0.0^{2,5}]octagermane (**19**) [41].

3.1. Synthesis and structures

The cross-coupling reaction of $\text{Cl}(i\text{-Pr})_2\text{GeGe}(i\text{-Pr})_2\text{Cl}$ and $\text{Cl}_2(t\text{-Bu})\text{GeGe}(t\text{-Bu})\text{Cl}_2$ with lithium in the presence of magnesium bromide gave the bicyclic ladder oligogermane **18** and the tricyclic ladder oligogermane **19** as air-stable colorless and pale yellow crystals, respectively (Scheme 14).

The structures of **18** and **19** were unequivocally established by X-ray crystallography (Fig. 4). The germanium framework of **18** has no crystallographically imposed symmetry. The two Ge_4 rings are fused with an angle of 113°. Both Ge_4 rings are folded and the dihedral angles are 19.6–21.6°. This may be the result of a compromise between the tendency to pucker, which alleviates the isopropyl–isopropyl eclipsing interaction, and electronically favored planar geometry.

The germanium framework of **19** had an *anti*-structure and was also twisted. Compound **19** was crystallographically isomorphous with the silicon analog, *anti*-1,2,5,6-tetra-*t*-butyl-3,3,4,4,7,7,8,8-octaisopropyltricyclo[4.2.0.0^{2,5}]-octasilane (**5**), and conformations of substituents were nearly identical. The average Ge–Ge bond length of 2.518(1) Å is considerably longer than the standard value (2.41 Å). There is no remarkable difference between the central Ge–Ge bond distances (average 2.519(1) Å) with those of the peripheral Ge–Ge bonds (average 2.517(1) Å). The dihedral angles for three Ge_4 rings were 22.6, 17.6, and 25.6°. It is noted that the structurally related *anti*-3,4,7,8-tetrachloro-1,2,3,4,5,6,7,8-octa-*t*-butyltricyclo[4.2.0.0^{2,5}]-octagermane has a similar geometry [40].

3.2. Electronic properties

In the UV–vis spectra of **18**, the absorption band has a shoulder at 297 nm (ε 1700), and **19** has the absorption maximum at 328 nm (ε 5000) and a shoulder at 359 nm (ε 2000). The blue shifts of absorption maxima were observed in **18** relative to 1,4-di-*t*-butyl-2,2,3,3,5,5,6,6-octaisopropylbicyclo[2.2.0]hexasilane (**20**; 317 nm) and in **19** relative to **5** (369 nm). On the other hand, the oxidation potentials of **18** (0.75 V vs. SCE, in CH_2Cl_2) and **19** (0.70 V) are significantly lower than those of silicon analogs (**20**; 0.98 V, **5**; 0.88 V). The results might suggest that both HOMO and LUMO levels of ladder oligogermanes are higher than those of corresponding ladder oligosilanes.

4. Comparison with octasilacubanes

In 1988, as the first example of the silicon polyhedranes, we synthesized [(*t*-BuMe$_2$Si)Si]$_8$ (**21**) [3]. Since then, the synthesis and properties of polyhedranes of Group 14 elements have been reported from several research groups [10], and we also reported the various reactions starting from stable octasilacubane, (ThexSi)$_8$

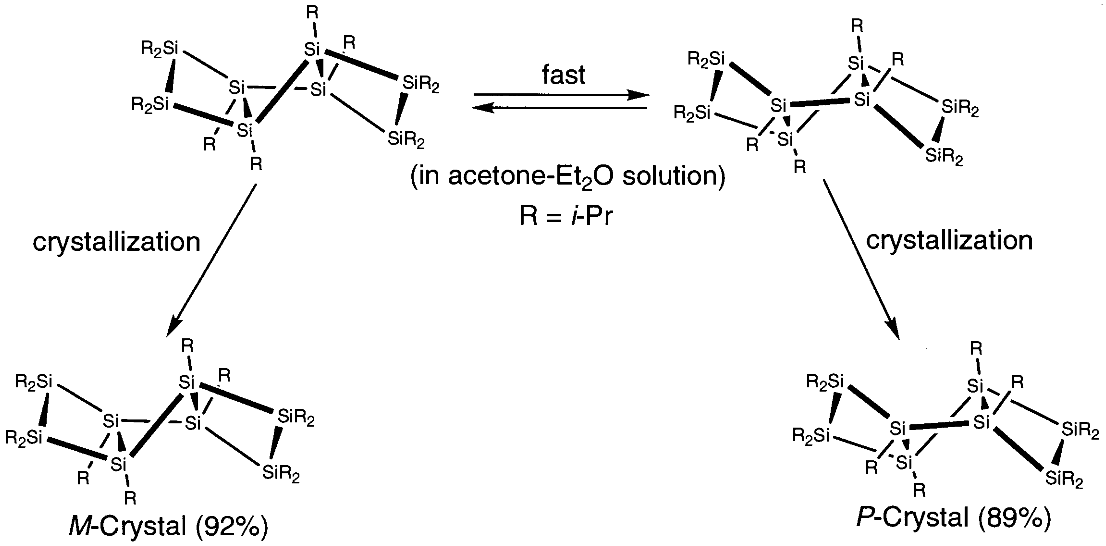

Scheme 13.

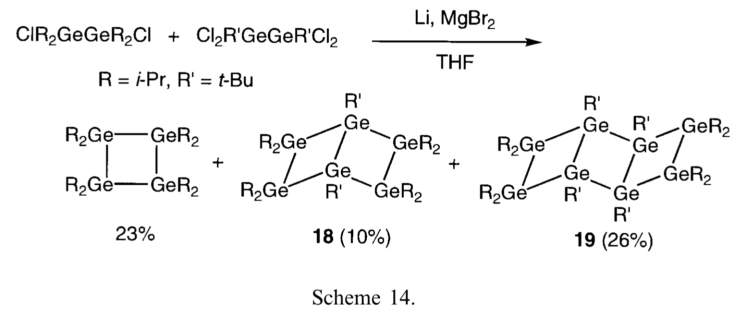

Scheme 14.

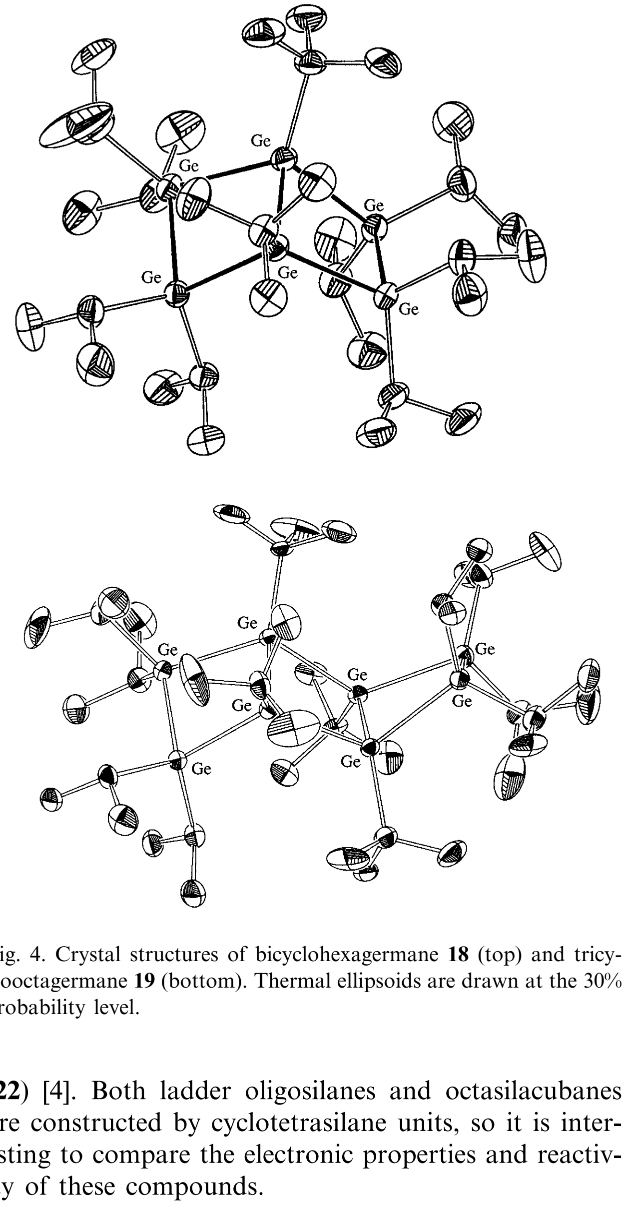

Fig. 4. Crystal structures of bicyclohexagermane **18** (top) and tricyclooctagermane **19** (bottom). Thermal ellipsoids are drawn at the 30% probability level.

(**22**) [4]. Both ladder oligosilanes and octasilacubanes are constructed by cyclotetrasilane units, so it is interesting to compare the electronic properties and reactivity of these compounds.

4.1. Synthesis and properties of octasilacubanes

Both octasilacubanes (**21** and **22**) were synthesized in a similar manner [3,4]. Thus, the reaction of t-BuMe$_2$SiSiBr$_3$ or ThexSiCl$_3$ with an excess amount of sodium in refluxing toluene gave pure octasilacubanes. Yields were 18% for **21** and 3% for **22**. In the case of silyloctasilacubane **21**, the reaction starting from Br$_2$(t-BuMe$_2$Si)SiSi(t-BuMe$_2$Si)Br$_2$ gave the optimized yield (24%). Octathexyloctasilacubane **22** is air-stable and soluble in hydrocarbons. In addition, it possesses low oxidation potential of 0.43 V (vs. SCE in CH$_2$Cl$_2$), which is traced back to the highly strained Si$_8$ framework. The most striking feature of **22** is that it could survive in the reversed-phase HPLC (eluent: THF–MeOH), which makes it possible to separate the reaction products. On the other hand, **21** also has a low oxidation potential of 0.40 V (vs. SCE in CH$_2$Cl$_2$). However, **21** is air-sensitive and oxidized easily.

4.2. Halogenation reaction

The chlorination of **22** with PCl$_5$ resulted in skeletal rearrangement with concomitant formation of stereoisomeric 4,8-dichlorooctakis(1,1,2-trimethylpropyl)tetracyclo[3.3.0.0^{2,7}.0^{3,6}]octasilanes (**23**) [42]. The three possible stereoisomers, *endo,exo*-**23**, *exo,exo*-**23**, and *endo,endo*-**23**, could be isolated in a yield of 37, 33, and 15%, respectively. A similar reaction occurs with bromine or iodine, and in each case, a mixture of three isomers was obtained. Reaction products are summarized in Scheme 15. These results are in good agreement with the halogenation reaction of the ladder oligosilane shown in Scheme 6.

When the mixture of three isomers of dihalosilane was treated with sodium in toluene, octasilacubane was regenerated. The yield was 70% from dichlorides, 68% from dibromides, and 45% from diiodides [43]. This

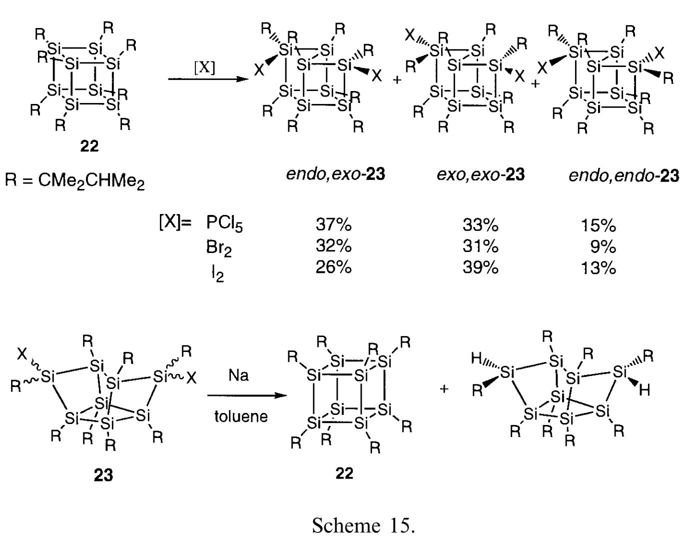

[X]=	endo,exo-23	exo,exo-23	endo,endo-23
PCl$_5$	37%	33%	15%
Br$_2$	32%	31%	9%
I$_2$	26%	39%	13%

Scheme 15.

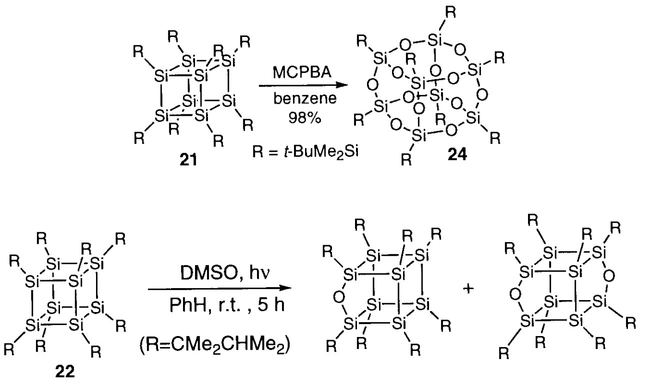

Scheme 16.

also resembles the regeneration reaction of the ladder oligosilane shown in Scheme 5.

4.3. Oxidation reaction

As mentioned above, silyloctasilacubane **21** is easily oxidized in air. The reaction of **21** with 14 equivalents of MCPBA in benzene gave octasilsesquioxane **24** (T_8) in 98% yield. A similar reaction from **22** gave only a complex mixture, which is explained by more steric hindrance in **22**. The photoreaction of **22** in DMSO gave mono- and dioxaoctasilacubanes [44]. The yields were 46% for monooxide and 39% for dioxide. The reaction pathway is shown in Scheme 16.

These reactions of octasilacubanes shown above indicate that ladder oligosilanes and octasilacubanes show similar reaction properties.

Acknowledgements

This work was supported by Grants-in-aid on Priority Areas (No. 09239103 and No. 10740287) from the Ministry of Education, Science, Sports, and Culture of Japan.

References

[1] (a) H. Matsumoto, T. Arai, H. Watanabe, Y. Nagai, J. Chem. Soc. Chem. Commun. (1984) 724. (b) H. Matsumoto, M. Minemura, K. Takatsuna, Y. Nagai, M. Goto, Chem. Lett. (1985) 1005. (c) H. Matsumoto, K. Takatsuna, M. Minemura, Y. Nagai, M. Goto, J. Chem. Soc. Chem. Commun. (1985) 1366. (d) H. Matsumoto, A. Sakamoto, Y. Nagai, J. Chem. Soc. Chem. Commun. (1986) 1768. (e) H. Matsumoto, N. Yokoyama, A. Sakamoto, Y. Aramaki, R. Endo, Y. Nagai, Chem. Lett. (1986) 1643. (f) S. Kyushin, H. Sakurai, H. Matsumoto, J. Organomet. Chem. 499 (1995) 235. (g) S. Kyushin, M. Kawabata, H. Sakurai, H. Matsumoto, M. Miyake, M. Sato, M. Goto, Organometallics 13 (1994) 795. (h) M. Unno, R. Tanaka, T. Kuribara, M. Saito, H. Matsumoto, Bull. Chem. Soc. Jpn. 70 (1997) 2749. (i) M. Unno, H. Masuda, H. Matsumoto, Bull. Chem. Soc. Jpn. 71 (1998) 2449. (j) R. Tanaka, M. Unno, H. Matsumoto, Chem. Lett. (1999) 595.

[2] (a) H. Matsumoto, H. Miyamoto, N. Kojima, Y. Nagai, J. Chem. Soc. Chem. Commun. (1987) 1316. (b) H. Matsumoto, H. Miyamoto, N. Kojima, Y. Nagai, M. Goto, Chem. Lett. (1988) 629.

[3] H. Matsumoto, K. Higuchi, Y. Hoshino, H. Koike, Y. Naoi, Y. Nagai, J. Chem. Soc. Chem. Commun. (1988) 1083.

[4] H. Matsumoto, K. Higuchi, S. Kyushin, M. Goto, Angew. Chem. Int. Ed. Engl. 31 (1992) 1354.

[5] (a) R. West, in: G. Wilkinson, G.A. Stone, E.W. Abel (Eds.), Comprehensive Organometallic Chemistry, vol. 2, Pergamon, New York, 1982 (Chapter 9.4). (b) R. West, in: P. Patai, Z. Rappoport (Eds.), The Chemistry of Organic Silicon Compounds, Part 2, Wiley, Chichester, UK, 1989 (Chapter 19).

[6] T. Tsumuraya, S.A. Batcheller, S. Masamune, Angew. Chem. Int. Ed. Engl. 30 (1991) 902.

[7] E. Hengge, R. Janoschek, Chem. Rev. 95 (1995) 1495.

[8] S. Kyushin, H. Matsumoto, Y. Kanemitsu, M. Goto, J. Phys. Soc. Jpn. Suppl. B 63 (1994) 46.

[9] (a) A. Sekiguchi, H. Sakurai, in: R. Steudel (Ed.), The Chemistry of Inorganic Ring Systems, Elsevier, New York, 1992 (Chapter 7). (b) A. Sekiguchi, H. Sakurai, Adv. Organomet. Chem. 37 (1995) 1.

[10] A. Sekiguchi, H. Sakurai, in: Z. Rappoport, Y. Apeloig (Eds.), The Chemistry of Organic Silicon Compounds, Wiley, Chichester, UK, 1998 (Chapter 2).

[11] R. West, A. Indriksons, J. Am. Chem. Soc. 94 (1972) 6110.

[12] For review concerning carbosilanes with cage and polycyclic structures, see G. Fritz, E. Matern, Carbosilane (Syntheses, Reactions), Springer-Verlag, Heiderverg, 1986.

[13] Recently, preparation and characterization of the novel cage polycarbosilanes, hexasilabicyclo[2.2.2]octanes, have been reported: M. Shimizu, N. Inamasu, Y. Nishihara, T. Hiyama, Chem. Lett. (1998) 1145.

[14] For the rings and cages consisting of alternating arrangement of P and Si atoms: G.M. Kollegger, U. Katzenbeisser, K. Hassler, C. Krüger, D. Brauer, R. Gielen, J. Organomet. Chem. 543 (1997) 103 and Refs. therein.

[15] (a) M.A. Miller, J.M. Schulman, J. Mol. Struct. (Theochem) 163 (1988) 133. (b) G. Mehta, M.B. Viswanath, G.N. Sastry, E.D. Jemmis, D.S.K. Reddy, A.C. Kunwar, Angew. Chem. Int. Ed. Engl. 31 (1992) 1488. (c) W. Li, M.A. Fox, J. Am. Chem. Soc. 118 (1996) 11752. (d) R.N. Warrener, G. Abbenante, C.H.L. Kennard, J. Am. Chem. Soc. 116 (1994) 3645.

[16] S. Kyushin, R. Tanaka, K. Hasegawa, K. Kanuma, M. Goto, H. Matsumoto, submitted.

[17] S. Kyushin, M. Kawabata, Y. Yagihashi, H. Matsumoto, M. Goto, Chem. Lett. (1994) 997.

[18] R. Tanaka, H. Matsumoto, submitted.

[19] S. Nagase, T. Kudo, J. Chem. Soc. Chem. Commun. (1988) 54.

[20] S. Kyushin, R. Tanaka, H. Matsumoto, submitted.

[21] However, the MM2 calculation of [10]ladderane predicted that the helical structure is slightly more stable than the planar structure (Ref. [15a]).

[22] H. Gilman, W.H. Atwell, G.L. Schwebke, J. Organomet. Chem. 2 (1964) 369.

[23] S. Kyushin, H. Yamaguchi, T. Okayasu, Y. Yagihashi, H. Matsumoto, M. Goto, Chem. Lett. (1994) 221 and Refs. therein.

[24] K. Kumar, M.H. Litt, J. Polym. Sci. Polym. Lett. Ed. 26 (1988) 25.

[25] S. Kyushin, H. Sakurai, H. Yamaguchi, H. Matsumoto, Chem. Lett. (1996) 331 and Refs. cited therein.

[26] (a) U. Burkert, N.L. Allinger, Molecular Mechanics, American Chemical Society, Washington, DC, 1982 (Chapter 4). (b) S. Chang, D. McNally, S. Shary-Tehrany, M.J. Hickey, R.H. Boyd, J. Am. Chem. Soc. 92 (1970) 3109.

[27] (a) H. Sakurai, T. Imoto, N. Hayashi, M. Kumada, J. Am. Chem. Soc. 87 (1965) 4001. (b) K. Tamao, M. Kumada, T. Sugimoto, J. Chem. Soc. Chem. Commun. (1970) 285. (c) K. Tamao, M. Kumada, M. Ishikawa, J. Organomet. Chem. 31 (1971) 17. (d) K. Tamao, M. Kumada, J. Organomet. Chem. 31 (1971) 35. (e) Y. Nakadaira, H. Sakurai, J. Organomet. Chem. 47 (1973) 61. (f) H. Sakurai, Y. Kamiyama, J. Am. Chem. Soc. 96 (1974) 6192. (g) B.J. Helmer, R. West, Organometallics 1 (1982) 1463. (h) I.S. Alnaimi, W.P. Weber, Organometallics 2 (1983) 903. (i) M. Weidenbruch, A. Schäfer, J. Organomet. Chem. 269 (1984) 231.

[28] S. Kyushin, H. Sakurai, H. Yamaguchi, M. Goto, H. Matsumoto, Chem. Lett. (1995) 815.

[29] S. Kyushin, R. Tanaka, K. Arai, A. Sakamoto, H. Matsumoto, Chem. Lett. (1999) 1297.

[30] S. Kyushin, Y. Yagihashi, H. Matsumoto, J. Organomet. Chem. 521 (1996) 413.

[31] R. Walsh, H.-D. Martin, M. Kunze, A. Oftring, H.D. Beckhaus, J. Chem. Soc. Perkin Trans. 2 (1981) 1076.

[32] S. Kyushin, A. Meguro, M. Unno, H. Matsumoto, Chem. Lett. (2000) 494.

[33] S. Kyushin, Y. Miyajima, H. Matsumoto, submitted.

[34] B.J. Helmer, R. West, Organometallics 1 (1982) 1458.

[35] (a) D.K. Kondepudi, R.J. Kaufman, N. Singh, Science 250 (1990) 975. (b) D.K. Kondepudi, K.L. Bullock, J.A. Digits, J.K. Hall, J.M. Miller, J. Am. Chem. Soc. 115 (1993) 10211. (c) D.K. Kondepudi, C. Sabanayagam, Chem. Phys. Lett. 217 (1994) 364.

[36] (a) R.E. Pincock, R.R. Perkins, A.S. Ma, K.R. Wilson, Science 174 (1971) 1018. (b) R.E. Pincock, K.R. Wilson, J. Am. Chem. Soc. 93 (1971) 1291. (c) K.R. Wilson, R.E. Pincock, J. Am. Chem. Soc. 97 (1975) 1474. (d) K.R. Wilson, R.E. Pincock, Can. J. Chem. 55 (1977) 889. (e) R.B. Kress, E.N. Duesler, M.C. Etter, I.C. Paul, D.Y. Curtin, J. Am. Chem. Soc. 102 (1980) 7709. (f) D.K. Kondepudi, J. Laudadio, K. Asakura, J. Am. Chem. Soc. 121 (1999) 1448.

[37] (a) M. Weidenbruch, A. Hagedorn, K. Peters, H.G. von Schnering, Angew. Chem. Int. Ed. Engl. 34 (1995) 1085. (b) M. Weidenbruch, A. Hagedorn, K. Peters, H.G. von Schnering, Chem. Ber. 129 (1996) 401.

[38] (a) M. Fujiki, J. Am. Chem. Soc. 116 (1994) 6017. (b) M. Fujiki, J. Am. Chem. Soc. 116 (1994) 11976. (c) H. Frey, M. Möller, K. Matyjaszewski, Macromolecules 27 (1994) 1814. (d) K. Obata, M. Kira, Macromolecules 31 (1998) 4666.

[39] R. Tanaka, S. Kyushin, M. Unno, H. Matsumoto, submitted.

[40] A. Sekiguchi, H. Naito, C. Kabuto, H. Sakurai, Nippon Kagaku Kaishi (1994) 248.

[41] R. Tanaka, S. Kyushin, M. Unno, H. Matsumoto, submitted.

[42] M. Unno, K. Higuchi, M. Ida, H. Shioyama, S. Kyushin, H. Matsumoto, M. Goto, Organometallics 13 (1994) 4633.

[43] M. Unno, H. Shioyama, M. Ida, H. Matsumoto, Organometallics 14 (1995) 4004.

[44] M. Unno, T. Yokota, H. Matsumoto, J. Organomet. Chem. 521 (1996) 409.